Research Article | Vol. 29, No. 21 / 11 Oct 2021 / Optics Express 33322
Optics EXPRESS

114 nm broadband all-fiber nonlinear polarization rotation mode locked-laser and time-stretch optical coherence tomography

HONGJIE CHEN,[1,2] YUJIA LI,[1,2] DONGMEI HUANG,[1,2,*] FENG LI,[2,3] CHAO LU,[2,3] AND P. K. A. WAI[2,3,4]

[1] *Photonics Research Centre, Department of Electrical Engineering, The Hong Kong Polytechnic University, Hong Kong SAR, China*
[2] *The Hong Kong Polytechnic University Shenzhen Research Institute, Shenzhen 518057, China*
[3] *Photonics Research Centre, Department of Electronic and Information Engineering, The Hong Kong Polytechnic University, Hong Kong SAR, China*
[4] *Department of Physics, Hong Kong Baptist University, Hong Kong SAR, China*
[*] *meihk.huang@polyu.edu.hk*

Abstract: We propose and demonstrate an all-fiber Er-doped mode-locked laser with a 3-dB spectrum of 114 nm by using nonlinear polarization rotation (NPR), which to the best of our knowledge is the first realization to date of such a broad spectrum without any spatial optical devices. The repetition rate and pulse width of the laser are 183.6 MHz and 3.7 ps, respectively. Such an all-fiber NPR mode-locked laser is then applied in time-stretch optical coherence tomography. The axial resolution is 12.1 μm. The all-fiber high speed broadband swept laser based on the time stretching technique has compact structure and high stability, which is a promising source for frequency metrology and high resolution optical coherence tomography.

1. Introduction

Optical coherence tomography (OCT), first demonstrated by D. Huang et al. in 1991, is a powerful technique for in-vivo, non-invasive and high-resolution cross-sectional imaging of biological tissues [1]. Swept source OCT (SS-OCT) adopts a swept laser and a single photodetector to acquire a time-resolved interference signal. SS-OCT has higher imaging speed when compared with time domain OCT which is hampered by the mechanical movement of the reference arm. SS-OCT also has higher resolution when compared with spectrum domain OCT which is limited by the resolution of the spectral detectors used such as the charge-coupled devices (CCD) or complementary metal-oxide-semiconductor (CMOS) [2–5]. A high speed swept laser with a broadband spectrum is the key to achieve high speed and high resolution imaging in SS-OCT systems.

A variety of swept lasers have been applied in the SS-OCT system. A conventional swept laser consists of a resonator which includes a gain medium and a fast tunable optical bandpass filter dynamically tuned to set the lasing wavelength [6,7]. The sweep rate is limited to kilohertz because lasing has to be built up from spontaneous emission in each round trip. By integrating all the components into a compact optical platform and adopting a MEMS filter, the cavity can be shortened to ~10 cm. Such a short-cavity swept laser can reach a sweep rate up to 200 kHz [8]. However, short laser cavities suffer from mode hopping, are relatively unstable, and have short coherence lengths [9]. Mode hopping can be avoided by combining vertical-cavity surface emitting lasers (VCSEL) with MEMS, which can generate MHz swept rate with long coherence length but the output power is low [10]. In 2006, a novel Fourier domain mode-locked fiber laser was proposed by inserting a long fiber delay in the cavity to store all the lasing signal, thus avoiding laser build-up from spontaneous emission in each round trip. The sweep

#438609 https://doi.org/10.1364/OE.438609
Journal © 2021 Received 27 Jul 2021; revised 17 Sep 2021; accepted 21 Sep 2021; published 29 Sep 2021

Optics EXPRESS

rate was increased to several hundred kilohertz or even megahertz if buffering is used [11–13]. Swept lasers utilizing mechanical tunable filters have long term stability problem, which can be mitigated by using inertia-free or passive swept mechanism.

Time stretching is a promising method to realize megahertz or even hundreds of megahertz swept lasers, overcoming the limitation of tunable filters [14–16]. In time stretching, a broadband mode-locked short pulse is broadened to a long chirped pulse by group velocity dispersion (GVD). The performances of the swept laser such as the sweep rate, sweep range and coherence are determined by the repetition rate, spectrum range and coherence, respectively, of the seed mode-locked fiber laser used. The main difficulty to obtain a high performance seed mode-locked fiber laser is that the gain bandwidth of rare earth doped fibers is normally limited to about 30 nm. Nonlinear spectral expansion, either inside or outside the laser cavity, can be used to obtain a bandwidth of more than 100 nm. Outside the laser cavity, supercontinuum generation in nonlinear fibers pumped by narrow bandwidth pulses could significantly expand the pulse spectra, but the coherence of the output signal is limited by modulation instability [17,18]. A flat broadband spectrum with 10-dB bandwidth of 100 nm is obtained from an polarization-maintaining figure-9 mode-locked fiber laser after nonlinear spectral expansion in an Erbium-doped fiber amplifier [16,19–20]. External spectral expansion however inevitably increases the complexity of the laser system. Dispersion and nonlinearity management inside the mode-locked fiber laser is a preferred and also an effective approach to obtain high power broadband pulses. Both figure-8 and figure-9 mode-locked fiber laser configurations with dispersion management have been demonstrated to be able to realize stable broadband ultrashort pulses [21–24]. However, ultrashort pulses with 3-dB spectral width up to 100 nm have not been demonstrated yet. Nonlinear polarization rotation (NPR) mode-locking, one of the popular passive mode-locked techniques, has been widely used to obtain broadband ultrashort pulses [15,25–33]. Short pulses with 3-dB spectral width of more than 100 nm have been demonstrated in dispersion-managed Er-doped fiber lasers [28–30]. These NPR-based mode-locked fiber lasers all utilized spatial optical devices such as half wave and quarter wave plates, which render practical applications of these lasers difficult. Although an all-fiber NPR Er-doped mode-locked fiber laser with a 10-dB bandwidth of 102 nm has been reported, the spectrum has a large slope and the 3-dB bandwidth directly from the fiber laser is only ~30 nm [15].

In this paper, we demonstrate an all-fiber mode-locked laser with a simple compact configuration, 114 nm broadband spectrum, 183.6 MHz repetition rate and high stability. The self-starting evolution dynamics of the mode locking is measured by using the dispersive Fourier transform technique. The high repetition rate broadband mode-locked fiber laser is then incorporated in an SS-OCT system utilizing time stretching which achieves both high resolution and high imaging speed. The rest of the paper is organized as follows. Section II describes the experimental setup and performances of the all-fiber mode-locked fiber laser and its applications in the SS-OCT system. Section III concludes the paper.

2. Experimental setup and results

2.1. Broadband all-fiber nonlinear polarization rotation mode-locked laser

Figure 1 shows the experimental setup of the proposed Er-doped fiber ring laser based on NPR mode-locking technique and the measurement system. Compared with other NPR mode-locked fiber laser with spatial optical devices, this laser cavity consists of only fiber components. The configuration is simple and compact. The total length of the laser cavity is ~1.12 m only, thus the laser is not sensitive to the ambient temperature variation when operating at room temperature. An optical integrated module consisting of a 20:80 optical coupler, a 980/1550 nm wavelength division multiplexer and a polarization dependent isolator is used to realize the pump coupling and 20% laser output. About 0.42 m of Er-doped fiber (nLIGHT Liekki Er80-8/125) with a dispersion of ~16.14 ps/nm/km at 1550 nm is used as the gain medium and pumped by a 980 nm

Optics EXPRESS

single mode laser diode. Dispersion management in the laser cavity is paramount in obtaining a broadband output spectrum. We use a section of about 0.11 m dispersion compensation fiber (DCF) with a dispersion of −166.1 ps/nm/km at 1545 nm to compensate the cavity dispersion to close to zero. Besides dispersion compensation, the polarization and nonlinearity in the laser cavity are also carefully controlled by optimizing the polarization state of the light by the two polarization controllers (PCs). The output spectrum is measured by an optical spectrum analyzer (ANDO, AQ-6315B, OPTICAL SPECTRUM ANALYZER). The repetition rate is determined by a photodetector, an oscilloscope (OSC, KEYSIGHT, DPO759SA-X 96204Q) and an electrical spectrum analyzer (ESA, KEYSIGHT, N9020B). The pulse width is measured by an autocorrelator (Femtochrome, FR-103HS). The dispersive Fourier transform (DFT) method is used to capture the dynamics of the mode-locking process to understand the mechanism of broadband spectrum generation. A section of 1.49 km single mode fiber, which is carefully calculated and measured by optical time domain reflectometry (ANDO, AQ7250) is used as the dispersion element in the DFT-based spectroscope. 20% of the output laser signal is used as self-clocking for the real-time oscilloscope and a high-speed photo-detector (PD, HP, 83440C LIGHTWAVE DETECTOR, DC-20 GHz) is used to acquire the time-stretched laser pulses.

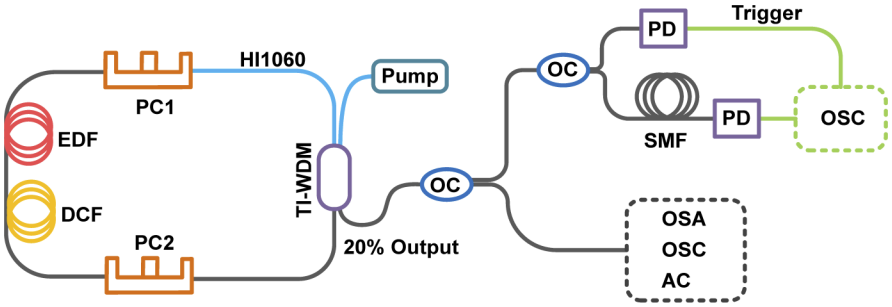

Fig. 1. Schematic diagram of the all-fiber mode-locked laser and the measurement system.

Pump power is a key parameter for mode-locking and nonlinearity management to realize flat broadband spectrum. When the pump power is 516 mW, a stable mode-locked pulse is obtained with a 3-dB spectral width of 40 nm at the center wavelength of 1560 nm. By further increasing the pump power to 1.1 W and carefully adjusting the polarization state of the light in the laser cavity, a flat ultra-broadband spectrum with a 3-dB and 10-dB spectral bandwidth of 114 and 160 nm respectively are obtained as shown in Fig. 2(a), which to the best of our knowledge is the broadest pulse bandwidth reported to date by an NPR-based all-fiber mode-locked laser. The generation of such a flat broadband spectrum is mainly the result of the precise dispersion and nonlinearity management of the fiber cavity. We manage the cavity dispersion by carefully adjusting the SMF length, enabling the fiber laser to operate from the anomalous dispersion regime where classical Kelly sidebands can be observed on the mode-locked spectrum to the normal dispersion regime with rectangular spectrum [28,34–35]. The total dispersion of the mode-locked fiber laser is ~0.00116 ps^2. Figure 2(b) shows that the adjacent pulse separation is 5.45 ns, which is consistent to the cavity length. Figure 2(c) shows the autocorrelation trace of the mode-locked pulse. The pulse width is determined to be ~3.7 ps by Gaussian fitting. The large chirped pulse can be compressed to femtosecond level with higher peak power outside the laser cavity. Figure 2(d) shows the RF spectrum of the mode-locked pulses. The signal-to-noise ratio (SNR) is ~80 dB at a resolution bandwidth of 10 kHz and the fundamental repetition rate is 183.6 MHz, indicating stable mode-locking operation [15,31–33].

The long-term spectral stability of the broadband mode-locked fiber laser is then investigated. The duration of the test is 9 hours and measurements are at 30-minute interval. The stability

Optics EXPRESS

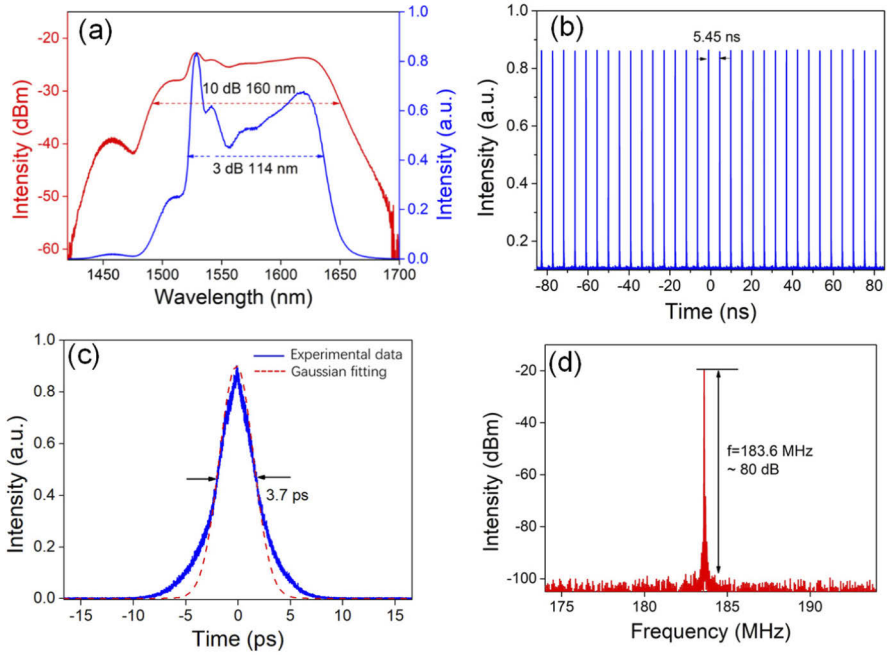

Fig. 2. Output characterization of the NPR-based broadband mode-locked fiber laser. The (a) optical spectra, (b) pulse train, (c) autocorrelation trace, and (d) RF spectrum.

test is conducted at room temperature and the pump power is fixed at 1.1 W. The PCs are not adjusted during the test. From Fig. 3(a), there are no obvious spectral fluctuations, and the central wavelength does not drift and remains around 1579 nm during the 9-hour test. Figure 3(b) presents the corresponding output power and the full-width-at-half-maximum (FWHM) pulse width. The output power is ~31 mW with a fluctuation of ~0.071 dB, indicating a good stability of the output power. The output spectrum has a 3-dB bandwidth of more than 110 nm throughout the 9-hour test period. We note that the spectral bandwidth can be affected slightly by environmental perturbations because the NPR-based mode-locked oscillator is polarization sensitive. After the 9-hour test, the decrease in the spectral width can be restored by carefully adjusting the polarization controllers without changing the pump power. The laser can also self-start, simply by turning off and on the pump laser without adjusting the PCs.

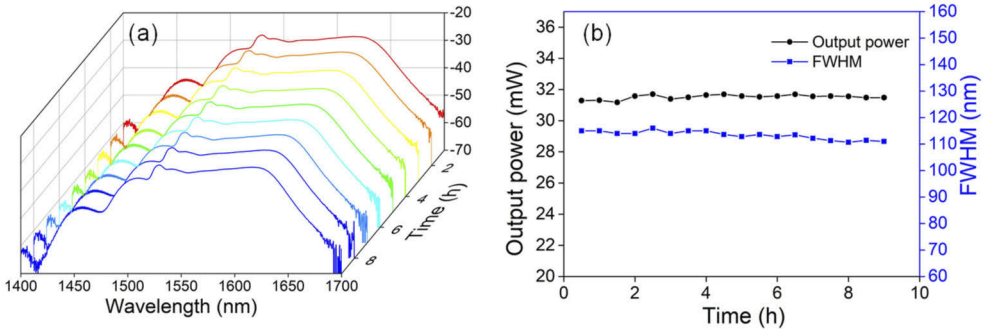

Fig. 3. The spectral stability test. The test duration is 9 hours and the corresponding output power as well as the 3-dB spectral width. Measurements were recorded every 30 minutes.

Optics EXPRESS

The transient dynamics of the mode-locking process is studied to demonstrate the generation of the broadband spectrum. The single-shot measurements of the buildup process of the broadband pulses, in both the temporal and spectral domains, are conducted by using the DFT technique as shown in Fig. 1. Figure 4(a) shows the temporal evolution dynamics including the growth of the pulse from the noise, relaxation oscillation and stable mode locking. The resolution is limited by the bandwidth and acquisition rate of the OSC. The oscillation stage lasts for ~32.7 μs, which is close to the relaxation time of the EDF. The oscillations then become stronger and the soliton starts to buildup. Figure 4(b) shows the spectral evolution which is similar to that of a previous study on soliton buildup dynamics in a dispersion management fiber laser [36], where the beating dynamics is first observed accompanied by the multipulse spectrum evolution induced spectral broadening. The complex pulse and energy evolution dynamics are related to the population inversion of the gain medium [37]. Figure 4(c) shows the zoom-in view from the 76,000-th to 76,300-th roundtrip. The effect of self-phase modulation (SPM) is clearly shown. The intensity at the central wavelength is the highest and gradually decreases from the central wavelength to both sides accompanied by spectral broadening. Finally, one pulse will absorb almost all the cavity energy and generate a stable time-domain profile and the weak pulse cluster will disappear as shown in Figs. 4(c) and 4(d). From the dynamics, strong amplification with 1.1 W pump power for the EDF can lead to strong SPM which in turn leads to the broadband spectrum, resulting in the observed 114 nm spectral bandwidth [38].

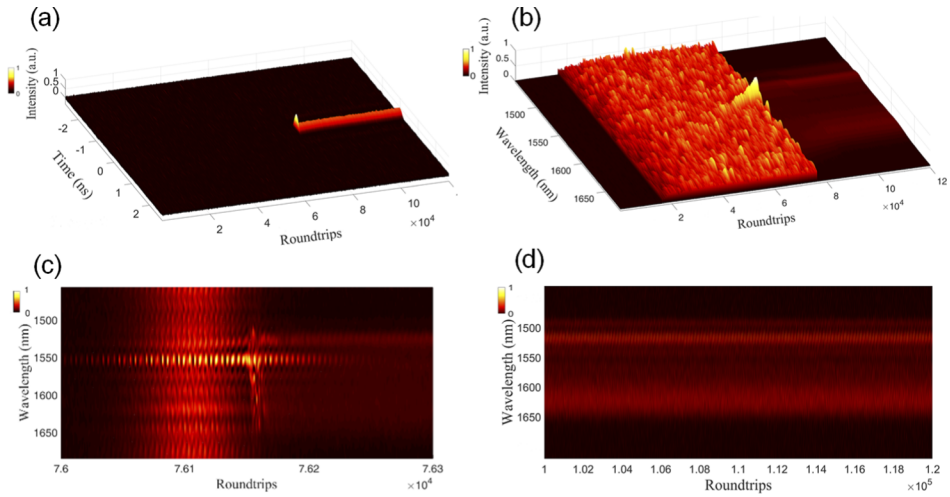

Fig. 4. Real-time measurements of the self-starting process of the broadband fiber laser. The (a) spatio-temporal dynamics and (b) the corresponding spatio-spectral evolution over 120,000 consecutive roundtrips. (c) The spatio-spectral evolution of 300 roundtrips from the 76,000-th to 76,300-th roundtrips showing the beating dynamics. (d) The spatio-spectral evolution of 20,000 roundtrips from the 100,000-th to 120,000-th round trips demonstrating stable mode-locking.

2.2. Time stretched swept laser and OCT imaging system

Time stretching an ultrashort broadband spectrum to a long chirped pulse by dispersive components such as single mode fiber, dispersion compensation fiber and chirped fiber Bragg grating (CFBG) is a promising method to realize high speed swept lasers. Figure 5 shows the schematic of an SS-OCT system in which a length of 1.49 km single mode fiber is used as the dispersive medium to stretch the output of a mode-locked fiber laser at a repetition rate of 183.6 MHz and spectral width of 114 nm. The swept signal after the SMF is then split by an optical coupler (OC, 10:90)

Optics EXPRESS

and transmitted to a Michelson interferometer. 10% of the light propagates through a circulator and is reflected by a homemade motorized reflective variable optical delay lines (VODLs) as the reference arm. 90% of the light propagates through the circulator and is then collimated by a collimator (Thorlabs, LA1509-C) and scanning mirrors (Thorlabs, GVS102) before finally focused on the sample. The galvo scanning system is driven by an arbitrary waveform generator (160 MHz Dual Channel Function, BK PRECISION) with a scanning speed of 500 Hz. The reflected light from the sample and the reference is then combined by a 50:50 optical coupler and detected by a 43-GHz bandwidth balanced photodetector (Finisar, BPDV2150R) and acquired by a real-time oscilloscope (OSC, KEYSIGHT, DPO759SA-X 96204Q) with a bandwidth of 62 GHz and a sampling rate of 160 GSa/s. To obtain the point spread function of the SS-OCT system, the 10:90 optical coupler is replaced by a 50:50 optical coupler and the sample arm is replaced by the reflective variable optical delay line (VODL). A portion of light from the mode-locked fiber laser is detected by a photodetector and used as the trigger signal for the OSC.

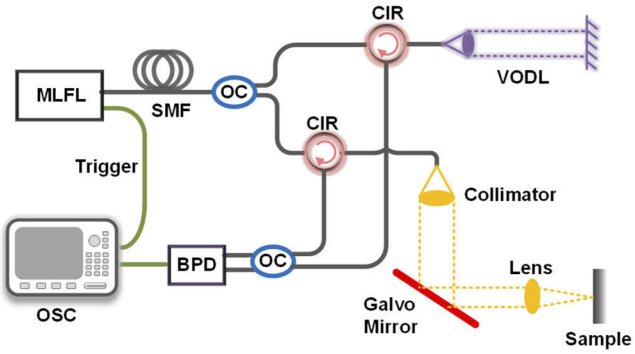

Fig. 5. A schematic diagram of the SS-OCT system.

Figure 6(a) shows the stretched pulse with about 4.5 ns pulse width which is consistent with the dispersion of the 1.49 km SMF. The temporal waveform has a similar profile with the spectrum shown by the blue curve in Fig. 2(a), which indicates that there is no nonlinear effect after the SMF. Figure 6(b) shows the interference fringes with modulations captured by the OSC. The modulations in the interference signal is caused by the optical path difference between the two arms of the Michelson interferometer, which will help to precisely obtain the depth information of the sample. By using the swept trace $\omega(t)$, the resampled interference signal in the frequency domain is obtained and then used in fast Fourier transform (FFT) with zero paddings to calculate the point spread function (PSF) as shown in Fig. 6(c). The starting point of each sampling period has been properly set to ensure the time to wavelength mapping is correctly resolved. The stable sweep trace, because of the stable seed mode locked laser used, will significantly reduce the need for recalibration in OCT systems. From Fig. 6(c), the axial resolution of the SS-OCT system is measured to be 12.1 μm in air by Gaussian fitting. The measured axial resolution is higher than those reported in the literature to date because of the use of the ultrabroadband swept laser which has a 3-dB bandwidth of 114 nm and 10-dB bandwidth of 160 nm. The high resolution SS-OCT system is then used to image two pieces of glass. As shown in Fig. 6(d), two layers of glass are clearly identified which correspond to the two reflecting surfaces of the glasses with 0.2 mm thickness. The different reflectivity of the glasses are also clearly identified with different demodulated intensities. In addition, microstructures of the cover glass are also clearly visible. SS-OCT imaging systems with such a high resolution will have significant applications in biomedical imaging and other industrial inspections such as jewelry and chips.

Optics EXPRESS

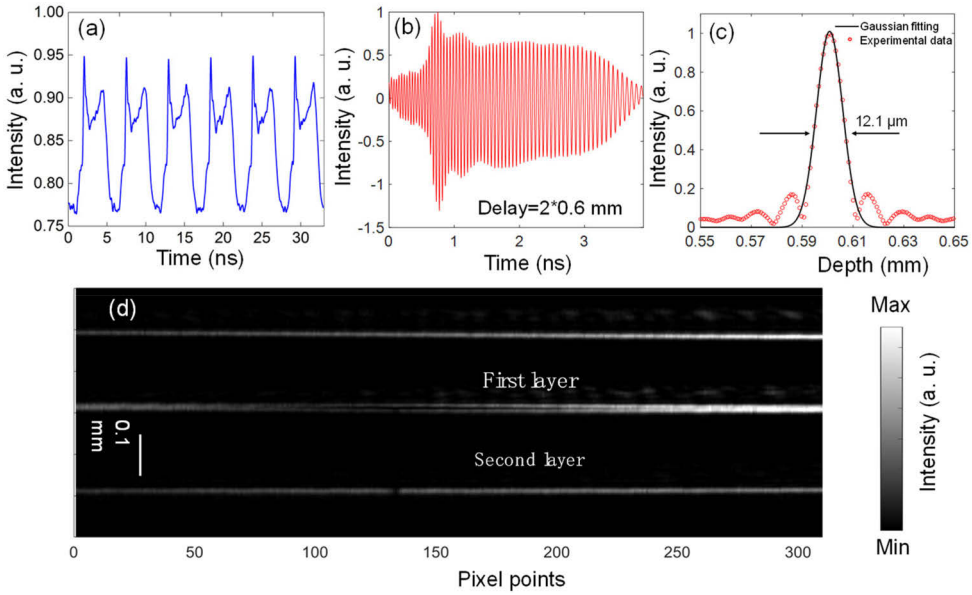

Fig. 6. (a) The pulse train stretched by the 1.49 km SMF. (b) A real-time single-shot interferogram generated by the SS-OCT system. (c) An axial resolution of 12.1 μm in air. (d) The OCT image of two pieces of cover glass overlapping together.

3. Summary

In summary, an all-fiber NPR mode-locked laser with repetition rate of 183 MHz and 3-dB spectral bandwidth of 114 nm and 10-dB of 160 nm is proposed and demonstrated by carefully managing the intra-cavity dispersion and nonlinearity. Because of the compact all-fiber configuration, the proposed fiber laser is stable with an 80-dB SNR and has only small power and spectral fluctuations in a 9-hour stability test. The dynamics of the mode-locked fiber laser is studied by using the DFT technique showing the mechanism of broadband spectrum generation, where strong amplification will lead to strong SPM and contribute to the broadband spectrum. The all-fiber mode-locked laser is then used as the seed laser to generate swept signal by time stretching technique and applied in a swept source OCT system. An axial resolution of 12.1 μm is obtained and two pieces of cover glass with microstructures are imaged. This novel all-fiber mode-locked swept laser with ultrabroadband spectrum and high stability provides a promising source for SS-OCT systems to obtain high speed and high resolution imaging in real time.

Funding. National Key Research and Development Program of China (2020YFB1805901); Science, Technology and Innovation Commission of Shenzhen Municipality (SGDX2019081623060558); Research Grants Council, University Grants Committee (PolyU152241/18E); Guangdong Basic and Applied Basic Research Foundation (2021A1515012544).

Disclosures. The authors declare no conflicts of interest.

Data availability. The data that support the plots within this letter and other findings of this study are available from the corresponding authors upon reasonable request.

References

1. D. Huang, E. Swanson, C. Lin, J. Schuman, W. Stinson, W. Chang, M. Hee, T. Flotte, K. Gregory, C. Puliafito, and A. Et, "Optical coherence tomography," Science **254**(5035), 1178–1181 (1991).
2. M. E. Brezinski, "Optical Coherence Tomography: Principles and Applications," (Academic Press, 2006), pp. 115–128.
3. V. J. Srinivasan and A. C. Smith, "*High-speed Fourier domain Optical Coherence Tomography by High-speed Fourier domain Optical Coherence Tomography*," Electr. Eng. (2008).

Optics EXPRESS

4. A. F. Fercher, W. Drexler, C. K. Hitzenberger, and T. Lasser, "Optical coherence tomography - principles and applications," Reports Prog Phys. **66**(2), 239–303 (2003).
5. A. G. Podoleanu, "Optical coherence tomography," J. Microsc. **247**(3), 209–219 (2012).
6. P. Qiao, K. T. Cook, K. Li, and C. J. Chang-Hasnain, "Wavelength-Swept VCSELs," IEEE J. Sel. Top. Quantum Electron. **23**(6), 1–16 (2017).
7. S. H. Yun, C. Boudoux, G. J. Tearney, and B. E. Bouma, "High-speed wavelength-swept semiconductor laser with a polygon-scanner-based wavelength filter," Opt. Lett. **28**(20), 1981–1983 (2003).
8. A.-H. Dhalla, K. Shia, and J. A. Izatt, "Efficient sweep buffering in swept source optical coherence tomography using a fast optical switch," Biomed. Opt. Express **3**(12), 3054–3066 (2012).
9. T. P. Butler, D. Goulding, S. Slepneva, B. O'Shaughnessy, S. P. Hegarty, G. Huyet, and B. Kelleher, "Experimental electric field visualisation of multi-mode dynamics in a short cavity swept laser designed for OCT applications," Opt. Express **27**(5), 7307–7318 (2019).
10. V. Jayaraman, G. D. Cole, M. Robertson, A. Uddin, and A. Cable, "High-sweep-rate 1310 nm MEMS-VCSEL with 150 nm continuous tuning range," Electron. Lett. **48**(1), 14 (2012).
11. R. Huber, M. Wojtkowski, and J. G. Fujimoto, "Fourier Domain Mode Locking (FDML): A new laser operating regime and applications for optical coherence tomography," Opt. Express **14**(8), 3225–3237 (2006).
12. T. Klein, W. Wieser, R. André, C. Eigenwillig, and R. A. Huber, "Multi-MHz retinal OCT imaging using an FDML laser," in *Biomedical Optics and 3-D Imaging* (OSA, 2012), p. BTu3A.90.
13. J. P. Kolb, T. Klein, M. Eibl, T. Pfeiffer, W. Wieser, and R. Huber, "Megahertz FDML laser with up to 143 nm sweep range for ultrahigh resolution OCT at 1050 nm," Proc. SPIE **9697**, 969703 (2016).
14. C. Lei, B. Guo, Z. Cheng, and K. Go da, "Optical time-stretch imaging: Principles and applications," Appl. Phys. Rev. **3**(1), 011102 (2016).
15. J. Kang, P. Feng, X. Wei, E. Y. Lam, K. K. Tsia, and K. K. Y. Wong, "102-nm, 44.5-MHz inertial-free swept source by mode-locked fiber laser and time stretch technique for optical coherence tomography," Opt. Express **26**(4), 4370–4381 (2018).
16. D. Huang, F. Li, C. Shang, Z. Cheng, and P. K. A. Wai, "100 MHz Reconfigurable Ultrafast Swept Source by Time Stretching of 100 nm Flat-top Spectrum," in ICOCN 2019 (IEEE, 2019), p. W2F.4.
17. H. Song, S. B. Cho, D. U. Kim, S. Jeong, and D. Y. Kim, "Ultra-high-speed phase-sensitive optical coherence reflectometer with a stretched pulse supercontinuum source," Appl. Opt. **50**(21), 4000–4004 (2011).
18. J. M. Dudley, S. Coen, G. Genty, and S. Coen, "Supercontinuum generation in photonic crystal fiber," Rev. Mod. Phys. **78**(4), 1135–1184 (2006).
19. D. Huang, F. Li, Z. Cheng, X. Feng, and P. K. A. Wai, "Ultrahigh-speed optical coherence tomography based on a 100 MHz and 100 nm swept source," arXiv preprint arXiv:2011.00514 (2020).
20. D. Huang, F. Li, C. Shang, Z. Cheng, and P. K. A. Wai, "Reconfigurable time-stretched swept laser source with up to 100 MHz sweep rate, 100 nm bandwidth, and 100 mm OCT imaging range," Photonics Res. **8**(8), 1360–1367 (2020).
21. J. W. Nicholson and M. Andrejco, "A polarization maintaining, dispersion managed, femtosecond figure-eight fiber laser, " Opt. Express **14**(18), 8160–8167, (2006).
22. J. Zhou, W. Pan, X. Fu, L. Zhang, and Y. Feng, "Environmentally-stable 50-fs pulse generation directly from an Er:fiber oscillator," Opt. Fiber Technol. **52**, 101963 (2019).
23. N. Nishizawa, H. Suga, and M. Yamanaka, "Investigation of dispersion-managed, polarization-maintaining Er-doped figure-nine ultrashort-pulse fiber laser," Opt. Express **27**(14), 19218–19232 (2019).
24. Z. Łaszczych and S. Grzegorz, "Dispersion management of a nonlinear amplifying loop mirror-based erbium-doped fiber laser," Opt. Express **29**(2), 2690–2702(2021) .
25. M. Hofer, M. E. Fermann, F. Haberl, M. H. Ober, and A. J. Schmidt, "Mode locking with cross-phase and selfphase modulation," Opt. Lett. **16**(7), 502–504 (1991).
26. K. Tamura, H. A. Haus, and E. P. Ippen, "Self-starting additive pulse mode-locked erbium fiber ring laser," Electron. Lett. **28**(24), 2226–2227 (1992).
27. H. A. Haus, K. Tamura, L. E. Nelson, and E. P. Ippen, "Stretched-pulse additive pulse mode-locking in fiber ring lasers: theory and experiment," IEEE J. Quantum Electron. **31**(3), 591–598 (1995).
28. L. E. Nelson, D. J. Jones, K. Tamura, H. A. Haus, and E. P. Ippen, "Ultrashort-pulse fiber ring lasers," Appl. Phys. B **65**(2), 277–294 (1997).
29. D. Ma, Y. Cai, C. Zhou, W. Zong, L. Chen, and Z. Zhang, "37.4 fs pulse generation in an Er:fiber laser at a 225 MHz repetition rate," Opt. Lett. **35**(17), 2858–2860 (2010).
30. Y. Lan, Y. Song, M. Hu, B. Liu, L. Chai, and C. Wang, "Enhanced spectral breathing for sub-25 fs pulse generation in a Yb-fiber laser," Opt. Lett. **38**(8), 1292–1294 (2013).
31. X. Li, W. Zou, G. Yang, and J. P. Chen, "Direct generation of 148 nm and 44.6 fs pulses in an Erbium-doped fiber laser," IEEE Photonics Technol. Lett. **27**(1), 93–96 (2015).
32. X. Wang, M. Sun, S. Yang, J. Pan, and S. Li, "Broadband Dispersion-Managed Dissipative Soliton and Structural Soliton Molecules in a Slight-Normal Dispersion Fiber Laser," IEEE Photonics J. **12**(6), 1–10 (2020).
33. J. Chen, X. Li, T. Li, Z. Zhan, M. Liu, C. Li, A. Luo, P. Zhou, K. K.-Y. Wong, W. Xu, and Z. Luo, "1.7-μm dissipative soliton Tm-doped fiber laser," Photonics Res. **9**(5), 873–878 (2021).
34. L. M. Zhao, D. Y. Tang, and J. Wu, "Gain-guided soliton in a positive group-dispersion fiber laser," Opt. Lett. **31**(12), 1788–1790 (2006).

Optics EXPRESS

35. W. H. Renninger, A. Chong, and F. W. Wise, "Dissipative solitons in normal-dispersion fiber lasers," Phys. Rev. A **77**(2), 023814 (2008).
36. D. D. Han, Z. Q. Hui, J. H. Xie, K. L. Ren, J. M. Guo, F. Zhao, J. Dong, D. D. Li, and X. J. Xin, "Single-shot observation of stretched-pulse buildup dynamics in an ultrafast fiber laser," Infrared Phys. Technol. **102**, 102984 (2019).
37. A. Chong, L. Wright, and F. Wise, "Ultrafast fiber lasers based on self-similar pulse evolution: a review of current progress," Rep. Prog. Phys. **78**(11), 113901 (2015).
38. D. Brida, G. Krauss, A. Sell, and A. Leitenstorfer, "Ultrabroadband Er: fiber lasers," Laser Photonics Rev. **8**(3), 409–428 (2014).